

ON THE VISCOSITY EFFECTS IN PROTON TRANSFER SYSTEMS. STRUCTURE AND PHOTOPHYSICS OF 2-(2'-HYDROXY-5'-METHYLPHENYL)-3,3-DIMETHYLINDOLE

Andrzej MORDZIŃSKI¹, Janusz LIPKOWSKI², Grażyna ORZANOWSKA¹

Institute of Physical Chemistry, Polish Academy of Sciences, 44 Kasprzaka, 01-224 Warsaw, Poland

and

Erich TAUER

Max Planck Institut für Biophysikalische Chemie, Abt. Spektroskopie, Am Fassberg, 3400 Göttingen, FRG

Received 5 June 1989

Temperature effects on fluorescence quantum yields and lifetimes of 2-(2'-hydroxy-5'-methylphenyl)-3,3-dimethylindole (HBDMI) and 2-(2'-hydroxyphenyl)benzoxazole (HBO) in the series of hydrocarbons were studied. The results obtained allowed us to examine the role of the viscosity in the electronically excited proton transfer (PT) systems. The large-amplitude torsional motions operate in the initially excited and PT forms. The X-ray determination of the crystal structure revealed that HBDMI is distorted from planarity in the crystalline state. We propose that solvent frictional forces effectively hinder the formation of the coplanar structure required for the barrierless proton transfer in the excited state.

1. Introduction

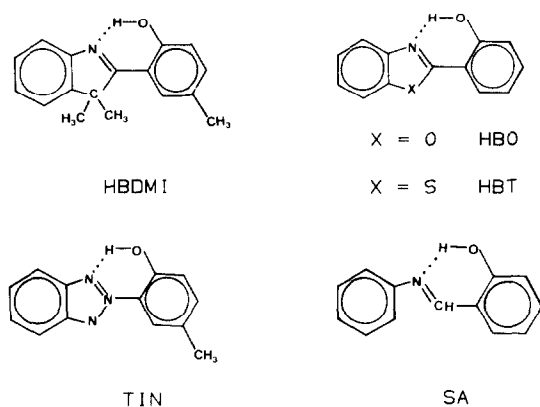
Since the pioneering works of Albert Weller [1] a large number of studies on the excited state proton transfer (PT) have been reported. Basing on the recent works applying time resolved picosecond techniques it can be concluded that PT processes within the singlet excited states manifold occur faster than in 5 ps [2,3], even at helium temperatures [4]. This fact is also in accord with the linewidth measurements of the matrix isolated PT systems [5]. As a consequence of the lack of energy barrier for PT in the excited state, it is very common to detect only the single, largely Stokes shifted fluorescence. However, this is not the general case; it was found in our laboratory [6-8] that a family of large π -electron systems exists, where PT reaction requires some thermal activation. The current interest concerns the dynamical aspect of photophysical processes associated with the excited state PT reaction.

One of the very often observed phenomena is the strong temperature dependence of the fluorescence intensity of the PT reaction product [9]. A variety of different descriptions of this effect were proposed. Felker et al. [10] have shown that the lowest excited singlet state of the initial form of methylsalicylate is strongly coupled to the radiationless decay channel, when the vibrational excess energy of about 1300 cm^{-1} is reached; this last value is in a good agreement with the activation energy for the nonradiative decay determined by Smith and Kaufmann [11]. The concept of the thermal excitation to the higher vibrational levels with larger nonradiative decay rates was recently discussed in connection with the "threshold behaviour", that was considered as a norm for not rigidly bonded systems [12].

Barbara, Brus and Rentzepis [13] have suggested, that the radiationless transition involves the torsional motion. This kind of intramolecular rotation results in a rapid rate for internal conversion [14,15]. Moreover, out-of-plane bending motions including intramolecular H-bond are known to operate as a decay channel in many similar systems [16,17].

¹ Department of Photochemistry and Spectroscopy.

² Department of Physicochemical Analytical Methods.



Scheme 1.

In the present work, we have focused our special attention on the role of solvent viscosity on the dynamical processes in the selected proton transfer systems. The results obtained provide the detailed arguments concerning the contribution of solvent friction in the PT reaction.

As an object of our studies we have chosen 2-(2'-hydroxy-5'-methylphenyl)-3,3-dimethylindole

(HBDMI) (see scheme 1). This particular molecule reveals strong deviations from planarity, so the vibrational relaxation is rather complicated because of the existence of many different low-frequency modes. Thus, we have performed also some parallel experiments with the model compound 2-(2'-hydroxyphenyl)benzoxazole (HBO), a relatively well known, planar system with only one C1–C7 torsional degree of freedom.

2. Experimental

2-(2'-hydroxy-5'-methylphenyl)-3,3-dimethylindole (HBDMI) was obtained from 1-(2-hydroxy-5-methylphenyl)2-methyl-1-propanone (according to the method of Kindler et al. [18]) and phenylhydrazine. The crude sample was purified by column chromatography and crystallized from methanol (m.p. 115.4°C). 2-(2'-hydroxyphenyl)benzoxazole (HBO) (Merck) was purified by sublimation, zone refining and HPLC. All solvents were purified by column SiO₂/Al₂O₃ chromatography.

The "fluorescence grade" of all solvents was

Table 1
Summary of data collection and structure analysis parameters

| | |
|---|--|
| molecule formula | C ₁₇ H ₁₇ O ₁ N ₁ |
| molecule weight | 251.33 |
| unit cell (Å) | <i>a</i> = 11.451(1) |
| <i>z</i> = 8 | <i>b</i> = 15.100(2) |
| | <i>c</i> = 15.850(2) |
| density (calculated) (g cm ⁻³) | 1.218 |
| space group | Pbca |
| radiation | CuK _α (graphite monochromatized) (CADY diffractometer) |
| absorption coefficient (cm ⁻¹) | 5.548 |
| crystal size (mm) | 0.25 × 0.36 × 0.45 |
| number of reflections | |
| measured | 2819 |
| unique | 2816 |
| used in the structure analysis | 2393 (<i>I</i> ≥ 2σ(<i>I</i>)) |
| final <i>R</i> value | |
| unweighted | 0.0495 |
| <i>R</i> = 1/[σ ² (<i>F</i>) + 0.0002 <i>FF</i> *] | 0.0489 |
| residual extrema in final difference map (e/Å) | < 0.2 and > -0.3 |

checked before the measurements. Emission and excitation spectra of HBDMI and HBO were performed in the temperature range between 300 and 100 K on a Jasný spectrofluorometer [19].

Fluorescence decay curves were recorded with the sampling technique using nitrogen-laser excitation. The digital data were directly transferred into the microcomputer for storage and analysis. The fluorescence lifetimes were determined using the least-squares method combined with the deconvolution of the laser pulse.

The crystals of HBDMI for X-ray measurements were obtained from concentrated cyclohexane solutions. The collected X-ray data and the structure refinement are given in table 1. The structure was solved by using a direct method, the MULTAN structure solution program [20] was used, and refined by a full matrix refinement procedure. The non-hydrogen atoms are refined with anisotropic thermal factors. Hydrogens were found from difference Fourier maps and included, in the final cycles of refinement, with isotropic thermal factors: the SHELX76 program [21] was applied for the refinement. The crystallographic structure data of HBDMI were applied as an input geometry for INDO/S calculations. The INDO/S semi-empirical method with the original parameterization of Ridley and Zerner [22] was applied. All singly excited configurations with the energy below 10 eV were used in the CI procedure.

3. Results

3.1. Crystal structure determination

Fig. 1 presents the conformation of the crystalline HBDMI with the bond distances obtained from the X-ray measurements. The standard deviations are less than 0.003 Å in bonds between nonhydrogen atoms and less than 0.03 Å in those involving H atoms. The fractional atomic coordinates for C, N, O and H atoms are presented in table 2. From these results we would like to point out two important facts. First, oxygen of O–H group is displaced by 0.05 Å from the plane of ring A (formed by the following atoms: C1, C2, C3, C4, C5 and C6). Secondly, the significant deviation from the molecular planarity mainly due to rotation about the C1–C7 bond was stated. The di-

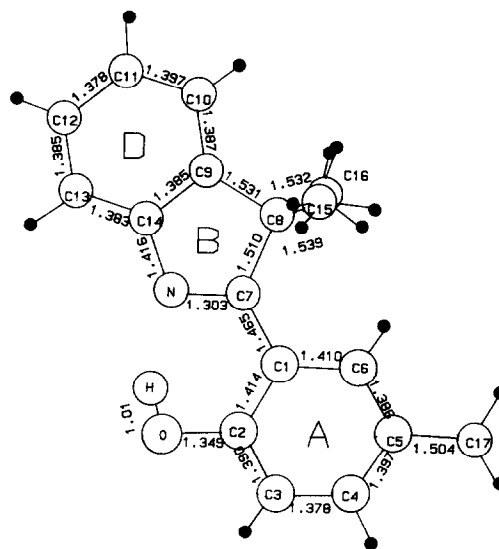


Fig. 1. Conformation and bond distances of crystalline HBDMI. The atomic numbering is related to table 2.

hedral angles formed by the least-squares planes A and B (N, C7, C8, C9 and C14) and A and D (C9, C10, C11, C12, C13 and C14) are 8.6° and 11.6°, respectively.

The complete structural data of HBDMI including refined thermal parameters, bond and torsional angles as well as dihedral angles formed by weighted least-squares planes have been deposited as supplementary material.

3.2. Photophysical observations

3.2.1. Steady-state measurements

Absorption, fluorescence and fluorescence excitation spectra of HBDMI measured in isopentane (IP) are shown in fig. 2. The excitation spectrum of the largely Stokes shifted fluorescence determined in the temperature range between 233 and 123 K agrees reasonably well with the absorption spectrum. It was assumed, that similarly to the parent molecules: 2-(2'-hydroxyphenyl)benzoxazole (HBO) [23] and 2-(2'-hydroxyphenyl)benzothiazole (HBT) [13] (see scheme 1), this fluorescence arises from the proton transferred species.

No fluorescence from the initially excited form was stated, although the radiative rate constant calcu-

Table 2

Fractional atomic coordinates ($\times 10000$) with estimated standard deviations (in parentheses) and mean temperature factors ($1000 B_{\text{eq}}$)

| Atom | x/a | y/b | z/c | B_{eq} |
|------|-----------|-----------|----------|-----------------|
| O | 10610(1) | 34(1) | 1009(1) | 5.02(0.03) |
| N | 9187(1) | 1321(1) | 899(1) | 3.47(0.03) |
| C1 | 9014(1) | 251(1) | 2002(1) | 2.90(0.03) |
| C2 | 10016(1) | -204(1) | 1712(1) | 3.42(0.03) |
| C3 | 10442(1) | -919(1) | 2171(1) | 4.03(0.04) |
| C4 | 9922(1) | -1175(1) | 2916(1) | 3.88(0.04) |
| C5 | 8933(1) | -742(1) | 3226(1) | 3.32(0.03) |
| C6 | 8488(1) | -46(1) | 2755(1) | 3.12(0.03) |
| C7 | 8605(1) | 1040(1) | 1553(1) | 2.83(0.03) |
| C8 | 7550(1) | 1621(1) | 1766(1) | 2.97(0.03) |
| C9 | 7718(1) | 2337(1) | 1112(1) | 3.12(0.03) |
| C10 | 7122(2) | 3123(1) | 970(1) | 4.23(0.04) |
| C11 | 7511(2) | 3674(1) | 320(1) | 4.65(0.05) |
| C12 | 8458(2) | 3442(1) | -169(1) | 4.47(0.04) |
| C13 | 9059(2) | 2659(1) | -32(1) | 4.07(0.04) |
| C14 | 8672(1) | 2120(1) | 616(1) | 3.19(0.03) |
| C15 | 7575(2) | 2013(1) | 2657(1) | 4.61(0.05) |
| C16 | 6402(2) | 1119(1) | 1603(1) | 4.48(0.04) |
| C17 | 8396(2) | -1012(1) | 4053(1) | 4.57(0.04) |
| Atom | x/a | y/b | z/c | U |
| H0 | 10177(26) | 557(13) | 748(18) | 1329(113) |
| H3 | 11176(19) | -1226(13) | 1928(12) | 729(58) |
| H4 | 10262(16) | -1673(12) | 3240(10) | 551(47) |
| H6 | 7755(15) | 247(11) | 2983(11) | 479(44) |
| H10 | 6424(17) | 3296(13) | 1357(12) | 701(55) |
| H11 | 7098(19) | 4252(15) | 193(14) | 783(62) |
| H12 | 8698(17) | 3856(13) | -595(12) | 686(58) |
| H13 | 9762(17) | 2480(14) | -347(12) | 658(53) |
| H151 | 7010(21) | 2532(1) | 2685(15) | 943(71) |
| H152 | 8397(22) | 2211(15) | 2846(14) | 885(71) |
| H153 | 7300(18) | 1565(15) | 3103(14) | 760(62) |
| H161 | 6333(18) | 620(15) | 1961(13) | 722(59) |
| H162 | 5685(20) | 1526(15) | 1706(12) | 756(61) |
| H163 | 6395(22) | 880(15) | 1003(16) | 940(77) |
| H171 | 8912(27) | -915(18) | 4553(18) | 1166(92) |
| H172 | 7629(23) | -667(18) | 4185(16) | 979(81) |
| H173 | 8395(25) | -1632(23) | 4134(18) | 1184(92) |

lated from the formula derived by Strickler and Berg [24] is rather large, $\approx 2.1 \times 10^8 \text{ s}^{-1}$. This observation points out that the photophysics of the primary form is controlled by the effective nonradiative deactivation channel, e.g., formation of proton transfer species. Moreover, as it will be shown below, internal conversion also contributes considerably in the overall depopulation of the initially excited form. The results of INDO/S quantum chemical calculations of

the transition energies are presented in fig. 2. The lowest excited singlet state of HBDMI was assigned as (π, π^*) (empty bar); the $S_2(n, \pi^*)$ transition (full bar) is predicted at about 3000 cm^{-1} above the S_1 . One must notice, that the S_1 - S_2 energy gap is in the case of HBDMI much lower than this for HBO, where $\Delta E \approx 9000 \text{ cm}^{-1}$. The spectroscopy of HBDMI is not complicated in the polar and protic solvents. This result is in opposition to the experimental data col-

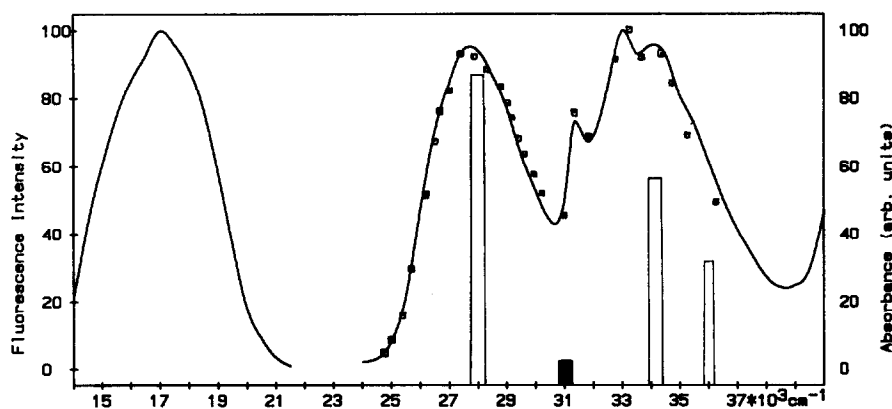


Fig. 2. Room temperature absorption and fluorescence spectra of HBDMI in isopentane. Dots: fluorescence excitation spectrum at 153 K, $\lambda^{\text{obs}} = 520$ nm. Bars represent the results of INDO/S calculation of transition energies for lowest excited singlet states. Empty bars: (π, π^*), full bars: (n, π^*).

lected for the HBO or HBT systems [3,25], where due to formation of the anion and/or intermolecular hydrogen bonding the distinct species in the ground state were detected; some of them do not lead to the PT form at all.

Fig. 3 presents the scheme of the virtual depopulation pathways of electronic excitation energy in the PT systems. An attempt to decode the contribution of the two temperature dependent nonradiative deactivation channels, k_{IC} and k'_{IC} (see fig. 3), temperature effects on the fluorescence lifetime (τ_{F}) as well as fluorescence quantum yield (ϕ'_{F}) of the PT final form was undertaken. Obviously, τ_{F} represents

exclusively the decay of the PT species, while ϕ'_{F} gives the insight into the efficiency of PT formation, e.g., the deactivation routes of the primary excited form. Table 3 presents the results of our measurements of the fluorescence quantum yields (ϕ'_{F}) of HBDMI and HBO in the different solvents, at room temperature. The investigations were limited to the hydrocarbons, what allows us to assume that the intermolecular interactions are comparable in the whole series. In the case of both systems ϕ'_{F} increases in the series from isopentane to decaline. These data strongly suggest that the photophysical parameters of both systems are strongly determined by the viscosity of the solvent.

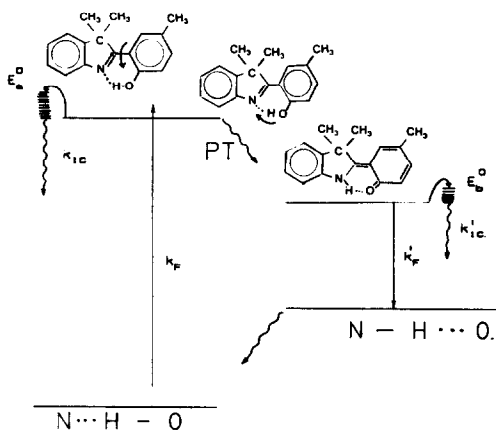


Fig. 3. Proton transfer photochemical cycle.

Table 3

Fluorescence quantum yield (ϕ'_{F}) of HBDMI and HBO at room temperature in the series of solvents of different viscosity (η); the dielectric constants (ϵ) of the pure solvents applied are listed, for comparison

| Solvent | System | | | |
|--------------|---|---|-------------|------------|
| | HBDMI $\phi'_{\text{F}} (\times 10^4)$ | HBO $\phi'_{\text{F}} (\times 10^2)$ | η (cP) | ϵ |
| IP | 2.8 | 1.9 | 0.22 | 1.84 |
| MCH/IP (1:1) | 4.1 | | | |
| MCH/IP (3:1) | 4.4 | | | |
| MCH | 5.5 | 3.0 | 0.74 | 2.02 |
| DE/IO (1:1) | 8.0 | | | |
| DE | 12.1 | 4.3 | 2.42 | 2.15 |

Also the temperature effect on the fluorescence intensities is a sensitive function of the solvent. For HBDMI the Arrhenius activation energies, extracted from the plot of $\ln(1/\phi'_F)$ versus $1/T$ are dependent on solvent and change between 2.6 ± 0.2 kcal/mole in isopentane and 3.9 ± 0.3 kcal/mole in decaline.

A similar trend was stated for HBO; here temperature dependence of $\ln(1/\phi'_F - 1)$ leads to the Arrhenius activation energies between 3.9 ± 0.3 and 5.5 ± 0.2 kcal/mole for isopentane and decaline, respectively.

3.2.2. Lifetime measurements

At room temperature the fluorescence lifetime of HBDMI in isopentane is as short as 14 ps [26]. It increases dramatically upon cooling and reaches a value of 3.6 ns at 77 K. The corresponding values of the fluorescence lifetime for HBO in 3-methylpentane are: $\tau'_F(293 \text{ K}) = 260 \text{ ps}$ [27] and $\tau'_F(77 \text{ K}) = 5.65 \text{ ns}$ [20]. We have studied the influence of viscosity on the fluorescence lifetime of HBDMI. The measurements were performed in five mixtures of organic hydrocarbons (isopentane (IP)), methylcyclohexane (MCH), isooctane (IO) and decaline (DE)), for which the very accurate viscosity data over the wide temperature range can be found in the literature [28,29]. The fluorescence decays are all characterized by fitting to the single exponential law with good accuracy. As a next step we have measured fluorescence lifetimes of HBO and HBDMI in different solvents as a function of temperature. The Arrhenius activation energies (E_b^{obs}) obtained from the plot $\ln(1/\tau'_F - 1/\tau'_0)$ versus $1/T$, are 3.6 ± 0.2 kcal/mole for HBO, practically independently of the solvent in agreement with the other observation reported above. In the case of HBDMI the striking result is that there is also no evident effect on E_b^{obs} and the solvent applied in spite of the viscosity dependence of τ'_F : $E_b^{\text{obs}} = 1.3 \pm 0.3$ kcal/mole and $E_b^{\text{obs}} = 1.6 \pm 0.2$ kcal/mole in isopentane and decaline, respectively.

We would like to point out the two important results presented on fig. 4. First, the direct correlation between the fluorescence lifetimes (τ'_F) of HBDMI and the macroscopic viscosity (η) of the solvent (see insert of fig. 4) was stated. Secondly the separation of the viscosity from the temperature effects was performed. Here, the radiationless rate constant of the PT form (k'_{IC}) was analyzed instead of the lifetime:

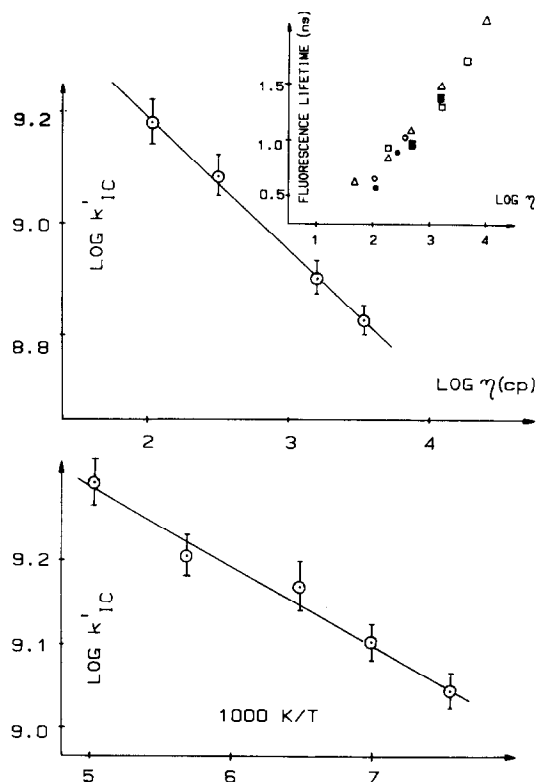


Fig. 4. (a) Variation of the nonradiative rate constant k'_{IC} of HBDMI in the PT form with solvent viscosity, at constant temperature ($T = 153 \pm 10 \text{ K}$). (b) Temperature dependence of the fluorescence decay rate of HBDMI at a constant viscosity of $150 \pm 20 \text{ cP}$. Least-squares fit gives the activation energies of 0.17 kcal/mol. Insert: correlation of the fluorescence lifetimes (τ'_F) of HBDMI with the solvent viscosity (η). (○) IP, (□) MCH/IP (1:1), (△) MCH/IP (3:1), (■) DE/IO (1:1) and (●) DE.

$1/\tau'_F - 1/\tau'_0 = k'_{IC}$, τ'_0 is derived from the temperature independent region, $\tau'_0 = \tau'_F(77 \text{ K})$.

Figs. 4a and 4b present variations of the radiationless rate constant of the PT form of HBDMI with the viscosity (at constant temperature, $T = 153 \pm 10 \text{ K}$) and temperature (at constant viscosity, $\eta = 150 \pm 20 \text{ cP}$). It is seen that in the case of HBDMI, both temperature and viscosity contribute to the overall photochemistry of the PT form.

In contrast, the fluorescence lifetime (τ'_F) of HBO seems to be insensitive to viscosity changes, e.g., τ'_F of HBO in decaline ($T = 203 \text{ K}$, $\eta = 110 \text{ cP}$), $3.3 \pm 0.2 \text{ ns}$, and in MCH/IP ($T = 203 \text{ K}$, $\eta = 5 \text{ cP}$), $\tau'_F = 3.0 \pm 0.3 \text{ ns}$. On the other hand, temperature plays an

important role, as exemplified by: $\tau_F' = 5.4 \pm 0.3$ ns in MCH/IP ($T = 133$ K, $\eta = 128$ cP).

4. Discussion

4.1. The structure of HBDMI in the crystalline state

It is generally accepted, that PT along the strong H bond is especially effective within the coplanar configuration, where the proton tunnelling distance is minimal. In fact, the crystal structure data of many H-bonded systems, e.g., TIN, HBO or HBT (see scheme 1) show, that they are almost perfectly planar – the interplanar angles do not exceed $0.5\text{--}0.9^\circ$ [30–32].

In contrast to these findings, in the case of HBDMI strong deviations from planarity were stated. These structural changes may partly relieve the repulsion interaction between H6 and H16 atoms. Acting in the same direction: in-plane deformation around C7 atom ($\angle \text{C1–C7–C8} = 127.7^\circ$) and rotation about C1–C7 bond of approximately 5.5° produce the separation of H6 and H16 atoms by 2.06 Å.

The second important structural aspect being in direct connection with proton transfer reactivity is the geometry of the intramolecular H bond. From X-ray data for HBDMI, one can read that the O–N distance in the O–H...N hydrogen bond is only 2.535 Å; this should be compared with the corresponding distances for some similar systems of exceptionally short, chelate type H bonds: TIN (2.615 Å) [30], HBT (2.605 Å) [31] or 2-chloro-N-salicylideneaniline (2.584 Å) [33]. Also other structural features states for HBDMI, e.g., O–H (1.01 Å), N...H (1.63 Å) and $\angle \text{O–H...N}$ (145°) can be treated as an indication of the particularly strong intramolecular H bond in this system [34].

4.2. Deactivation mechanism of HBDMI in the primary excited form

One of the striking experimental features of HBDMI is that τ_F' and ϕ_F' are not mutually proportional (ϕ_F' depends more on temperature).

Assuming the irreversibility of PT reaction in the excited state, the following equation holds for fluorescence quantum yield (ϕ_F') of PT form:

$$\phi_F' = \phi_{PT} \phi_F^{\text{int}} = \phi_{PT} k_F' \tau_F', \quad (1)$$

where $\phi_{PT} = k_{PT} / (k_F + k_{IC} + k_{PT})$ is the yield of the PT process, ϕ_F^{int} is the intrinsic fluorescence quantum yield of the PT form, and k_{PT} and k_{IC} are rate constants of nonradiative deactivation pathways of the initially excited form: proton transfer and internal conversion, k_F' and τ_F' are radiative rate constant and fluorescence lifetime of PT form, respectively (see fig. 3).

In order to detect the photophysical processes operating in the primary excited, “normal” form it is convenient to employ the τ_F' / ϕ_F' ratio. It can be shown that:

$$\tau_F' / \phi_F' = A(k_{IC} / k_{PT} + B), \quad (2)$$

where $A = 1 / k_F'$ and $B = 1 + k_F / k_{PT}$ are according to the reasonable assumption of temperature independent terms.

As the temperature dependences of τ_F' and ϕ_F' are not identical, also $\tau_F' / \phi_F' = 1 / \phi_{PT} k_F'$ is a function of temperature and/or viscosity, namely it decreases upon cooling. Thus, as k_F' is in many similar PT systems suspected to have neither temperature nor viscosity dependence, we propose that the effect observed reflects the change of the efficiency of the formation of proton transfer species.

In general one can expect that out-of-plane torsional motions, strongly dependent on the viscosity of the solvent, do influence the distance of the centers between which the ESPT reaction takes place. Obviously, this should be reflected in the PT rate constant (k_{PT}). Recently, Lee, Yardley and Hochstrasser [35] have shown that ESPT rates in TIN in alcohols are controlled by the solvent friction in the system where proton translocation is mediated by the solvent molecule. However the fact, that $\phi_{PT} = k_{PT} / (k_{PT} + k_{IC} + k_F)$ increases upon cooling, implies that in the case of HBDMI the temperature effect is mainly carried by internal conversion process (k_{IC}) of the primary, H-bonded form.

Recently, the importance of this nonradiative deactivation channel was discussed by Goeller et al. [36] for internally H-bonded TIN. To rationalize the temperature effect on τ_F' / ϕ_F' ratio the authors have postulated an intermediate excited species of the configuration similar to this of the twisted intramolecular charge transfer state [37,38].

In our case this hypothesis seems to be rather unapplicable. The phenyl ring of HBDMI is a part of the π -electron system and the extent of delocalization is a function of the phenyl torsional angle. As a consequence of the loss of the planarity via the rotation around C1–C7 bond the overlap between the π -electron subunits decreases; obviously, this should imply the increase of the ($\pi\pi^*$) transition energies. Indeed, in the INDO/S calculations we have reproduced this effect – the significant destabilization of all lowest excited singlet states was stated. Thus, one should expect that for HBDMI the TICT-like configuration is not a probable intermediate on the pathway between the initial and proton transferred form.

The Arrhenius activation energies (E_a^{obs}) extracted from the dependence $\ln(\tau_F'/\phi_F')$ versus $1/T$ (fig. 5) correlate with the mean activation energy for viscous flow E_η (fig. 6). The correlation obtained suggests that the mechanism of radiationless deactivation of the initial form is controlled by frictional forces in the solvent.

It was assumed that in the present case, the following phenomenological expression [39] holds: $k_{\text{IC}} = F(\eta) \exp(-E_a^0/RT)$. Here, $F(\eta)$ is indirectly a function of temperature through the temperature dependence of η : $\eta(T) = \eta_0 \exp(E_\eta/RT)$, where E_η is the apparent activation energy of solvent viscosity. If we accept, that at higher viscosities the empirical relation $F(\eta) = C\eta^{-\alpha}$ is fulfilled [40], then $k_{\text{IC}} = C\eta_0^{-\alpha} \exp(-E_a^{\text{obs}}/RT)$ and $E_a^{\text{obs}} = E_a^0 + \alpha E_\eta$, where E_a^0 is the intrinsic activation energy and $0 < \alpha < 1$.

One can expect that the temperature independent terms in eq. (2) are negligible in comparison to the $k_{\text{IC}}/k_{\text{PT}}$ ratio. From the plots of $\log(\tau_F'/\phi_F')$ versus $\log \eta$ (fig. 5) was found the straight line with the best fit for $\alpha = 0.35 \pm 0.1$, both for decaline and methylcyclohexane/isopentane; the reasonably good fit supports the fact that indeed the functional form: $k \approx \eta^{-\alpha} \exp(-E_a^0/RT)$ is applicable in the present case. Table 4 presents the activation parameters for HBDMI in its initial form; the direct separation of the intrinsic activation energy of the nonradiative process (E_a^0) and the viscosity dependent contribution is achieved. The intrinsic activation energy of ≈ 0.34 kcal/mole (119 cm^{-1}) corresponds reasonably to a torsional C–phenyl motion and should be compared with the frequency of 121 cm^{-1} calculated by Warshel for this mode [41]. One should notice,

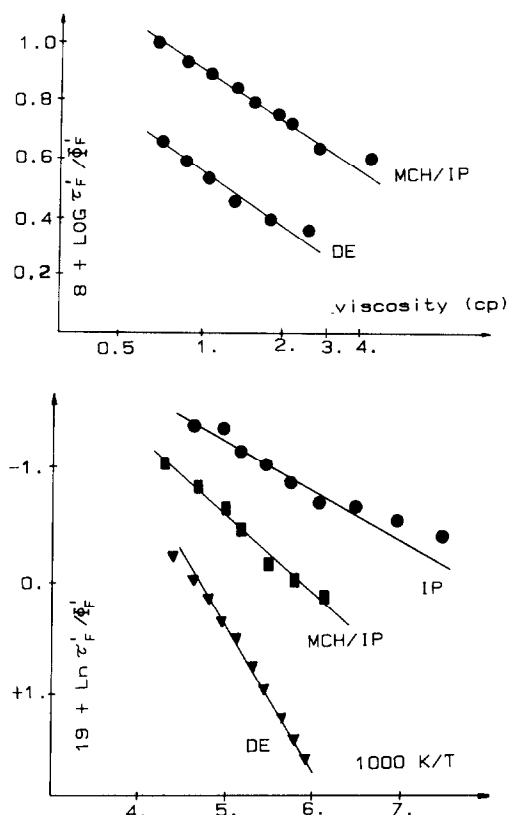


Fig. 5. (a) A $\log(\tau_F'/\phi_F')$ versus $\log \eta$ plot for HBDMI in MCH/IP and decaline. The curve drawn through the experimental data gives a good fit to the empirical relation $k_{\text{IC}} \approx \eta^{-\alpha}$, $\alpha = 0.35 \pm 0.1$. (b) Temperature dependence of τ_F'/ϕ_F' . Arrhenius activation energies (E_a^{obs}) of the nonradiative process (k_{IC}) of the N...H–O form.

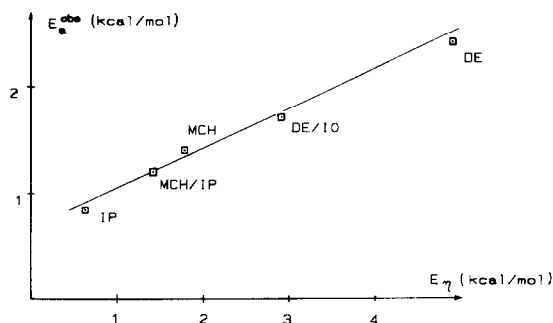
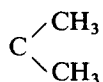


Fig. 6. Correlation between the Arrhenius activation energies (E_a^{obs}) of nonradiative process (k_{IC}) and the solvent viscosity activation energies (E_η).

Table 4
Thermal activation parameters (in kcal/mole) for the primary excited N...H–O form of HBDMI

| Solvent | E_a^{obs} | E_η | E_a^0 |
|--------------|--------------------|----------|---------|
| isopentane | 0.85 | 1.6 | 0.29 |
| MCH/IP | 1.2 | 2.4 | 0.36 |
| MCH | 1.4 | 3.05 | 0.33 |
| DE/isooctane | 1.7 | 3.9 | 0.34 |
| decaline | 2.4 | 5.9 | 0.33 |

that the macroscopic viscosity definitely influences the efficiency of formation of PT species in the case of HBDMI. This fact may suggest that



vibrations cooperate with the torsional motion of the molecule.

4.3. Radiationless decay channel of the PT species

The temperature dependence of fluorescence decay time is commonly described using the formula: $1/\tau_F = k'_F + k'_0 + k'_{IC}(T)$, where $k'_F + k'_0$ represents the sum of the radiative and the nonradiative temperature independent rate constants.

The radiationless transitions active in depopulation of PT species were recently widely discussed for many similar molecules. Woolfe et al. [3] and El-saesser et al. [25] have noticed the significant decrease of the fluorescence lifetime of HBO and HBT, when the dielectric constant of the solvent increases. Smith and Kaufmann [11] have found for methylsalicylate the empirical relationship between the nonradiative decay rates and the dielectric constant of the solvent.

According to the low-temperature $T_n \leftarrow T_1$ absorption data of HBDMI [42] we can conclude that triplet state formation via intersystem crossing plays a minor role in the deactivation mechanism. The non-radiative deactivation rate constant can be expressed approximately as $k'_{IC}(T) = A \exp(-E_b^{\text{obs}}/RT)$.

The plots of k'_{IC} versus $1/T$ give the satisfactory straight lines both for HBO and HBDMI. In the case of HBO we have obtained $E_b^{\text{obs}} = 3.6 \pm 0.2$ kcal/mole. The Arrhenius parameters are typical for many other

PT systems, e.g., methylsalicylate, $E_b^{\text{obs}} = 3.7$ kcal/mole [11], TIN, $E_b^{\text{obs}} = 3.98$ kcal/mole [30] and HBT, 4.0 kcal/mole [13]. In contrast, for HBDMI E_b^{obs} is only 1.6 kcal/mole. Our results for HBDMI give additional strong evidence supporting the idea of the role of intramolecular rotation in the radiationless deactivation channel. The direct correlation between $1/\tau'_F$ and $\log \eta$ (fig. 4) obtained for HBDMI in the series of hydrocarbons can be understood as a direct indication, that in this particular system the viscosity factors play an important role in the relaxation mechanism.

The internal barrier E_b^0 of the nonradiative process was extracted by plotting $\log k'_{IC}$ versus $1/T$ for $\eta = \text{constant}$ (fig. 4b), for a series of hydrocarbons. If the variations of E_b^0 from solvent to solvent are small, the isoviscosity plots should yield E_b^0 independently of the solvent applied and/or of the particular viscosity selected.

The intrinsic activation energy calculated from the isoviscosity plot is 60 ± 10 cm⁻¹. Since this isoviscosity plot was constructed from only a few points, the absolute value of E_b^0 is somehow uncertain. However, the result can be treated as a strong indication that the observed activation energy of nonradiative process, in the PT form $E_b^{\text{obs}} = 560$ cm⁻¹ (1.6 kcal/mole) is mostly due to solvent hindrance of large amplitude motion associated with the radiationless transition. This mechanism can modify the fluorescence decay channel of HBDMI in its proton transferred form.

5. Conclusion

HBDMI strongly deviates from planarity in its crystal state. In the condensed phase the system undergoes effective excited state proton transfer (ESIPT). Experimental studies of HBDMI in a series of hydrocarbons allow us to separate the effect of temperature and viscosity on radiationless transition in the PT system. The viscosity appears in the kinetic relations for radiationless transition both for the primary excited and PT forms.

For the PT species the direct correlation between the fluorescence lifetimes of HBDMI and the bulk viscosity of the solvent was stated. For the primary excited form the torsional C–phenyl motion operates

in the radiationless decay channel. We infer, that the solvent frictional forces control formation of the coplanar structure is required for the barrierless ES IPT.

Acknowledgement

Words of encouragement and helpful discussions with Professor Anna Grabowska are acknowledged. This work was done under project CPBP 01.19 and CPBR 3.20.

References

- [1] A. Weller, *Z. Electrochem.* 60 (1956) 1144.
- [2] T. Elsaesser and W. Kaiser, *Chem. Phys. Letters* 128 (1986) 231.
- [3] G.J. Woolfe, M. Melzig, S. Schneider and H. Dörr, *Chem. Phys.* 77 (1983) 217.
- [4] B. Dick and N.P. Ernstring, *J. Phys. Chem.* 91 (1987) 4261.
- [5] D.-J. Jang, G.A. Brucker and D.F. Kelley, *J. Phys. Chem.* 90 (1986) 6863.
- [6] A. Mordziński, A. Grabowska, W. Kühnle and A. Krówczyński, *Chem. Phys. Letters* 101 (1983) 291.
- [7] A. Mordziński, A. Grabowska and K. Teuchner, *Chem. Phys. Letters* 111 (1984) 383.
- [8] A. Mordziński and W. Kühnle, *J. Phys. Chem.* 90 (1986) 1455.
- [9] S.Y. Nagaoka, *J. Photochem. Photobiol. A* 40 (1987) 185.
- [10] P.M. Felker, Wm.R. Lambert and A.H. Zewail, *J. Phys. Chem.* 77 (1982) 1605.
- [11] K.K. Smith and K.J. Kaufmann, *J. Phys. Chem.* 82 (1978) 2286.
- [12] P.M. Felker and A.H. Zewail, in: *NATO ASI Series, Vol. 127. Application of Picosecond Spectroscopy in Chemistry*, ed. K.B. Eisenthal (Reidel, Dordrecht, 1984).
- [13] P.F. Barbara, L.E. Brus and P.M. Rentzepis, *J. Am. Chem. Soc.* 102 (1980) 2786, 5617.
- [14] E.P. Ippen, A. Bergman and C.V. Shank, *Chem. Phys. Letters* 38 (1976) 611.
- [15] G. Oster and N. Nishijima, *J. Am. Chem. Soc.* 78 (1956) 1581.
- [16] H. Inoue, M. Hida, N. Nakashima and K. Yoshihara, *J. Phys. Chem.* 86 (1982) 3182.
- [17] G. Calzaferri, H. Gugger and S. Leutwyler, *Helv. Chim. Acta* 59 (1976) 1969.
- [18] K. Kindler, H. Oelschläger and P. Henrich, *Archiv Pharmazie* 287 (1954) 210.
- [19] J. Jasny, *J. Luminescence* 17 (1978) 149.
- [20] P. Main, S.J. Fiske, S.E. Hull, L. Lessinger, G. Germain, J.P. Declereq and M.M. Woolfson, *MULTAN* 11/82, University of York, York, UK (1982).
- [21] G.M. Sheldrick, *SHELX76*, University of Cambridge, Cambridge, UK (1976).
- [22] J.E. Ridley and M.C. Zerner, *Theoret. Chim. Acta* 32 (1973) 111.
- [23] A. Mordziński and A. Grabowska, *Chem. Phys. Letters* 90 (1982) 122.
- [24] S.J. Strickler and R.A. Berg, *J. Chem. Phys.* 37 (1962) 814.
- [25] T. Elsaesser and T. Schmetzer, *Chem. Phys. Letters* 140 (1987) 293.
- [26] N. Tamai, private communication.
- [27] G.J. Woolfe, M. Melzig, S. Schneider and F. Dörr, in: *Springer Series in Physical Chemistry, Vol. 43. Picosecond Phenomena. III* (Springer, Berlin, 1986) p. 2309.
- [28] G.A. von Sallis and H. Labhard, *J. Phys. Chem.* 72 (1968) 293.
- [29] H. Lesche, D. Klemp and B. Nickel, *Z. Physik. Chem. NF* 141 (1984) 239.
- [30] G. Woessner, G. Goeller, P. Kollat, J.J. Stezowski, M. Hauser, U.K. Klein and H.E.A. Kramer, *J. Phys. Chem.* 88 (1984) 5544.
- [31] P. Stenson, *Acta Chem. Scand.* 24 (1970) 3729.
- [32] J. Lipkowski, unpublished results.
- [33] J. Bregman, L. Leisnowitz and K. Osaki, *J. Chem. Soc.* (1964) 2086.
- [34] G.M.J. Schmidt, *J. Chem. Soc.* (1964) p. 2014.
- [35] M. Lee, J.T. Yardley and R.M. Hochstrasser, *J. Phys. Chem.* 91 (1987) 4621.
- [36] G. Goeller, J. Rieker, A. Maier, J. Stezowski, E. Daltrozzo, M. Neuroiter, H. Port, M. Weichmann and H.E.A. Kramer, *J. Phys. Chem.* 92 (1988) 1452.
- [37] Z.R. Grabowski, K. Rotkiewicz, A. Siemiarczuk, D.J. Cowley and W. Baumann, *Nouv. J. Chim.* 3 (1979) 443.
- [38] W. Rettig, *Angew. Chem.* 98 (1986) 969.
- [39] S.H. Courtney and G.R. Fleming, *J. Chem. Phys.* 83 (1985) 215.
- [40] S.P. Velsko and G.R. Fleming, *J. Chem. Phys.* 76 (1982) 2553.
- [41] A. Warshel, *J. Chem. Phys.* 62 (1975) 214.
- [42] K.H. Grellmann, private communication.